Food & Function

Encapsulation and release of curcumin using intact milk fat globules delivery system

Journal:	*Food & Function*
Manuscript ID	FO-ART-03-2019-000489.R1
Article Type:	Paper
Date Submitted by the Author:	27-Jul-2019
Complete List of Authors:	Alshehab, Maha; University of California Davis, Food Science and Technology Nitin, Nitin; University of California Davis, Food Science and Technology

Encapsulation and release of curcumin using intact milk fat globules delivery system

Maha Alshehab[a], Nitin Nitin[a,b]

[a] Department of Food Science and Technology, University of California-Davis, Davis, CA 95616, United States. E-mail address: alshehab@ucdavis.edu

[b] Department of Biological and Agricultural Engineering, University of California-Davis, Davis, CA 95616, United States. E-mail address: nnitin@ucdavis.edu

1. Introduction

Bioactive compounds are defined as components with health promoting qualities that are naturally present in small quantities in food or produced *in vivo* upon digestion [1]. Bioactive compounds are often encapsulated to: a) deliver higher dosage in order to achieve desired biological effect, b) stabilize and protect the compound/s during manufacturing, storage, and delivery, and c) modulate the release and bioaccessibility of the bioactives. Curcumin is one of the most widely researched food grade bioactives in recent years. Curcumin is isolated from the rhizome of the herb *Curcuma longa* (turmeric). It is a hydrophobic polyphenolic compound with a log *P* (octanol/water partitioning coefficient) value of approximately 4.3 [2, 3]. Curcumin has been extensively researched for its various physiological activities, including anti-inflammatory, anti-oxidant, anti-cancer, and anti-microbial effects [4-10]. Based on its hydrophobicity and susceptibility to hydrolytic and oxidative damage, curcumin is often incorporated in food and drug products in an emulsified form.

Lipid-based delivery systems such as liposomes, nanoemulsion, and particles stabilized emulsions are commonly used for encapsulation of hydrophobic bioactives. Many of these lipid based encapsulation approaches require the addition of chelators and/ or antioxidants to reduce oxidation [11-13], and surfactants and emulsifiers to stabilize these colloidal particles [14, 15]. With increasing demand for more natural products without the addition of exogenous preservatives and stabilizers, there is growing interest in using natural systems such as cell-based carriers for the encapsulation of bioactives, including systems such as yeast and yeast cell wall carriers [16-20]. Such approaches capitalize on the

advantages of natural carriers, such as: the abundance of compositional and structural diversity, relative low cost, and intrinsic physiological compatibility.

This study investigated the utilization of the naturally occurring lipid-based structure, milk fat globules (MFGs). MFGs are synthesized via a complex process in the mammary epithelial cells [21], and are composed of a triglyceride core stabilized in an aqueous medium via multilayer lipoprotein membrane known collectively as milk fat globule membrane (MFGM). MFGs are distinguished from other cellular lipid bodies by their secretion process where cytoplasmic lipid droplets are enveloped by the apical plasma membrane resulting in formation of a unique complex MFGM that is enriched with various bioactive proteins, lipids, and other functional molecules [22, 23].

MFGs were considered for encapsulation due to their distinct compositional and structural features as well as wide availability, and a relative low cost. Milk fat that resides in the core of the globules is one of the most complex natural lipid with relatively higher concentrations of saturated fats than common emulsions [24, 25]. This could potentially retard the rate of lipids oxidation and consequent degradation of lipid soluble compounds [26]. Furthermore, the presence of MFGM have been reported to modulate lipolysis and release of encapsulate compounds [27]. Compositionally, MFGM possess excellent emulsification properties that are attributed to the unique mixture of many health beneficial phospholipids and proteins [28, 29].

This study investigated the use of isolated MFGs as carrier for the lipophilic bioactive compound, curcumin. Firstly, partitioning and encapsulation of curcumin in MFGs was confirmed microscopically. Follows, evaluation of the loading kinetics and encapsulation efficiency. Lastly, *in vitro* gastrointestinal release of encapsulated

curcumin was evaluated and correlated with changes in structural properties of MFGs carrier using particle size measurements and fluorescence imaging. In summary, this study provides a novel approach to encapsulate and deliver curcumin using MFGs as a carrier. The results of this study can provide understanding to develop novel value added products using a combination of polyphenolics and MFGs.

2. Materials and methods

2.1 Materials

Raw whole bovine milk was procured from local markets (Organic Pastures, Fresno, CA, U.S.A.). Nanopure distilled water (16 MΩ-cm) obtained using Millipore Milli-Q RG water purification system (Billerica, MA, U.S.A.). Ethanol (200 proof, KOPTEC), curcumin (Curcumin from curcuma longa (Turmeric)), tetrahydrofuran (THF), calcium chloride, potassium phosphate monobasic, bile salts, pepsin from porcine gastric mucosa, and lipase type II from porcine pancreas were obtained from Sigma-Aldrich (St. Louis, MO, U.S.A.). Slide-A-Lyzer G2 dialysis cassettes (3.5K MWCO), chloroform, hydrochloric acid, and sodium chloride were purchased from Thermo Fisher Scientific Inc. (Pittsburgh, PA, U.S.A.).

2.2 Methods

2.2.1 Isolation of milk fat globules

Raw milk was used within 3-4 days of purchasing during which it was stored at 4° C. MFGs were isolated using a modified form of the method by Gallier *et al.* (2010) [30]. In summary, raw milk was diluted using water (9:1 water to milk ratio). The diluted solution

was centrifuged at 3000 x *g* for 5 minutes; the cream layer was collected and dispersed in water to create 10% w/v suspension.

2.2.2 Quantification of milk fat in cream

Raw cream that was separated following the method stated in section 2.2.1 was used for the quantification of oil content per gram of raw cream. A 10% w/v cream was dispersed in water and homogenized using a hand-held disperser (ULTRA TURRAX, IKA works, Wilmington, NC, USA) at 11,000 rpm for 2 min. Fat was then extracted using chloroform at 5:1 homogenized cream to chloroform ratio, followed by centrifugation at 10,000 x *g* for 30 min at room temperature. The two immiscible phases were separated. Acidity of the aqueous phase adjusted to pH 4.5 using 1M HCl to precipitate remaining MFGM proteins and associated serum proteins. A final extraction of oil from the acidified aqueous phase was carried by adding chloroform to the acidified aqueous phase in the ratio of 1:25, followed by centrifugation at 10,000 x *g* for 10 min at room temperature. Chloroform extracts were combined and the solvent was removed under vacuum at room temperature for 24 h. Mass of the isolated lipid from the sample was measured gravimetrically. Measurements were completed in triplicated from independent raw milk samples.

2.2.3 Loading of curcumin in milk fat globules

Curcumin solution in ethanol was prepared at 2 mg/mL concentration. Aliquots of curcumin ethanolic solution were added to 10% w/v MFGs in water suspension and incubated for 10 min. Concentrations of added curcumin, as well as the v/v % of added

ethanol were adjusted as shown in Table 1. Incubation was completed in the dark to prevent photodegradation of curcumin. To study the kinetics of curcumin encapsulation, a fixed concentration of curcumin and ethanol were added to the aqueous suspension of raw cream, and incubation time was adjusted from 10-60 min at 10 min intervals. Encapsulations measurements were conducted in triplicates.

2.2.4 Extraction and quantification of curcumin encapsulated in milk fat globules

At the end of the incubation period, encapsulated curcumin was extracted from MFGs using THF at 1:10 volume ratio of cream suspension to THF. The mixture was then vortexed rigorously, followed by centrifugation at 16,000 x *g* for 10 min. Curcumin concentration was then measured using a UV–vis spectrophotometer (GENESYS 10S Series, Thermo Scientific, Pittsburgh, PA, USA) where λ_{max} of curcumin in THF was detected at 422 nm. Blanks samples of MFGs treated with ethanol were used to subtract background absorbance caused by MFGs components. A standard curve of curcumin in THF was used to convert relative absorbance units to concentration units. Curcumin containing samples were kept covered throughout the extraction and measurements steps. The encapsulation efficiency was calculated as follows:

$$\%EE = \frac{C_E}{C_T} \times 100$$

where C_E is the mass of curcumin extracted from MFGs, and C_E is the mass of curcumin added initially. The loading capacity was calculated as follows:

$$LC = \frac{C_E}{MF}$$

where C_E is the mass of curcumin extracted from MFGs, and MF is the mass of milk fat in MFGs suspension.

2.2.5 Fluorescence imaging of curcumin encapsulated in milk fat globules

A representative MFGs sample loaded with 600 μg curcumin/g raw cream as described in the section 2.2.3 was examined under a microscope using a 40× oil immersion objective (Olympus UPlanFL, 40x/1.30 oil, Olympus Inc., Center Valley, PA, USA). Fluorescence images were obtained using an inverted optical microscopy, Olympus IX-7 (Olympus Inc., Center Valley, PA, USA). The images were acquired using an excitation filter: 480/30 nm, and emission filter: 570/60 nm. The camera exposure time for image acquisition was set to 100 ms.

2.2.6 Release of curcumin from milk fat globules under simulated gastric digestion conditions

MFGs samples loaded with curcumin at 600 μg curcumin/g raw cream were used for the simulated gastric digestion measurements. Simulated gastric digestion was carried in a dialysis cassette with a molecular weight cut off of 3500 Da. MFGs suspension was combined with the simulated gastric fluids (SGF) in the dialysis cassette suspended in a 1L of enzyme-free SGF [31]. SGF was prepared according to the method reported by Sarkar *et al.* (2009) [32] where 5 g/L sodium chloride solution was acidified to pH 1.2 starting using 12.1 M HCl. Fine adjustments of the solution's pH were accomplished using 1M of HCl or NaOH. SGF was then stored at 37° C. When needed the pH was further corrected to account for temperature effects.

Nine milliliter of MFGs suspension (at 37° C), and 1 mL of SGF (at 37° C) containing additional 0.018 g NaCl and 0.032 g pepsin, were combined in a dialysis cassette. The cassette containing MFGs sample was then allowed to float and rotate in a beaker containing 1 L of enzyme-free SGF, with the aid of a magnetic stirrer and a stir plate set at approximately 450 rpm. This arrangement allows the released compound and degraded MFGs structures to diffuse out of the cassette as a result of concentration gradient. Equilibration of curcumin concentration in the two systems (inside and outside of the dialysis cassette) is not expected to occur over the course of digestion time (2 h) due to a large excess (100 fold) of the outer chamber volume and limited water solubility of curcumin. The simulated gastric system was maintained at 37±2° C for the 2 h duration of digestion. A hundred microliter aliquots were collected from the cassette every 30 min; the concentration of curcumin was measured using the previously described method in the section 2.2.4. Reported results are the average measurements of three independent runs. Additional 20 μL aliquot was collected and examined microscopically in order to study morphological changes of MFGs structure. Fluorescence imaging of curcumin was completed using the same procedure detailed in section 2.2.5.

2.2.7 Release of curcumin from milk fat globules under simulated intestinal digestion conditions

Simulated intestinal digestion was conducted using as a modified procedure based on an earlier reported study by Tikekar *et al.* (2013) [31]. In summary, simulated intestinal fluid (SIF) comprised of 0.05 M potassium dihydrogen phosphate solution, 6.66 mg/mL

calcium chloride, and 50 mg/mL bile salts. The addition of calcium chloride in the SIF causes some aggregation of bile salts. These aggregates were removed via centrifugation. The supernatant was removed and pH of the supernatant was adjusted to 7.5. The solution was equilibrated to 37° C, and 20 mg/mL of lipase was added directly prior to initiating the digestion protocol.

The SIF was mixed with the MFGs suspension (held at 37° C) at 1:1 volumetric ratio and incubated in a shaking incubator at 37° C and 95 rpm for a total of 3 h. Separate tubes were designated for each time point. At each time point (data were collected every 30 min for a total of 3 h), approximately 20 μL aliquot were collected for imaging purposes to study morphological changes of MFGs structure following the method of section 2.2.5. The SIF/MFGs mixture was centrifuged at 25° C and 47,808 x *g* for 30 min using Sorvall RC6^{+} Centrifuge, SS-34 fixed angel rotor (Thermo Scientific, Waltham, MA, USA). Release was defined as the measured concentration of curcumin in the transparent micellar phase. The concentration of curcumin in the micellar phase was measured based on UV-vis absorption at 425 nm. The micellar phase sample from digested control MFGs suspension served as a blank. Reported results are the average measurements of three independent runs.

2.2.8 Particle size measurements of milk fat globules during simulated gastrointestinal digestion conditions

Changes in MFGs particle size distribution during the digestion process was observed using Mastersizer 2000 particle analyzer (Malvern Instruments, Worcestershire, UK). The instrument was set to the following variables: particle refractive index = 1.45,

particle absorption index = 0.0, dispersant (Milli-Q water) refractive index = 1.33, model: general purpose spherical. Measurements were made using independent triplicate samples per time point. Furthermore, the milk fat globules were isolated from two different batches of milk. Thus, each time point reading had 6 independent measurements.

2.2.9 Statistical analysis

Statistical analysis was completed using Microsoft Excel 2010 (Microsoft Inc., Bellevue, WA, USA). Statistical significance was carried out using one-way ANOVA followed by post hoc Tukey's analysis to determine significant difference between groups. Significance values were reported with a 95% confidence interval, i.e. $p < 0.05$. Experimental data were collected in triplicates unless stated otherwise.

3. Results:

3.1 Encapsulation of curcumin in intact milk fat globules

Encapsulation of curcumin in MFGs was achieved by co-incubation of MFGs with a water-ethanol mixture containing curcumin. The partitioning of curcumin in MFGs was first validated microscopically. Fig. 1.A and B show bright field and fluorescence images of MFGs with curcumin, respectively. Fig. 1.A illustrates intact MFGs after incubation with water-ethanol mixture containing curcumin. The imaging results indicate MFGs maintain shape and integrity of the globules upon incubation with the aqueous solution containing ethanol and curcumin. Further validation of membrane integrity is illustrated in supplementary data, Fig. 1. Fig. 1.B shows uniform distribution of curcumin endogenous fluorescence, corresponding to localization of the compound in the

lipid core region of MFGs. These results demonstrate permeation of curcumin through the MFGM to the lipid core of MFGs.

To identify the influence of incubation time on the encapsulation efficiency and loading capacity, the incubation time was varied between 10-60 min as described in the section 2.2.3. Encapsulation efficiencies (EE%) as a function of incubation time for a fixed concentration of curcumin are shown in Table 1. EE% of curcumin in MFGs ranged between 57% and 66%. Using one-way ANOVA followed by Tukey's post hoc test, a small, yet statistically significant difference in EE% of curcumin in MFGs was observed after 50 min of incubation, compared to other time points tested in this study. In fact, this value was also the lowest calculated EE%. Due to limited influence of extended incubation time on EE% of curcumin in MFGs, incubation time of 10 min was selected for the following experiments.

The results in Table 2 present the EE% and LC of curcumin in MFGs as a function of increasing curcumin concentration (200-2000 μg/g of raw cream) in the aqueous phase, for a fixed incubation time of 10 min. As a result of increasing curcumin concentration, the ethanol concentration in the system increased from 1 to 10% v/v. The results show significant increase ($p<0.05$) in LC with an increase in the concentration of curcumin in the aqueous phase. The LC value increased from 368 μg/ g milk fat to 1186 μg/ g milk fat, representing a 3 fold increase, with an increase in curcumin concentration while the EE% did not change significantly except at 5% v/v ethanol solution. The EE% ranged from 59% to 66% for all the conditions tested for these set of experiments.

3.2 Effect of simulated gastric digestion on milk fat globules carriers

To study the release of encapsulated curcumin, the delivery system was evaluated using *in vitro* simulated digestion conditions with appropriate electrolytes and enzymatic composition, temperature and pH conditions [33-35]. Physical changes of MFGs were measured using fluorescence microscopy and particle size analysis. Release of encapsulated compound during gastric and intestinal phases was studied independently to allow for comprehensive understanding of the digestive events.

Fig. 2 shows the release of curcumin from MFGs under simulated gastric digestion. A small fraction, approximately 27%, of total curcumin encapsulation in MFGs was released after 2 h of incubation under simulated gastric conditions. Most of this release was observed during the first 30 min of incubation under gastric conditions. Additional release of curcumin (from 30-150 min) was not statistically significant ($p>0.05$).

Microscopic images of MFGs under simulated gastric digestion are shown in Fig. 3. After 30 min of gastric digestion, MFGs appeared intact as shown in Fig. 3.A. However at the end of the digestion period (2 h), irregular boundaries of lipid droplets were observed. These boundaries are highlighted with the red arrows in Fig. 3.C. Throughout the digestion time, fluorescent images of encapsulated curcumin show localization in the lipid pool of the MFGs (Fig. 3.B and D). Table 3 shows changes in particle size during gastric digestion. Statistically significant ($p <0.05$) increase in MFGs size is recorded compared to initial particle size prior to gastric digestion. Fig. 4 shows shift in the distribution of MFGs diameter at the end of the digestion period (2h) to larger values without noticeable difference in the overall shape of the distribution curve.

3.3 Effect of simulated intestinal digestion on milk fat globules carriers

Release of curcumin from MFGs as a result of simulated intestinal digestion is illustrated in Fig. 5. The first recorded time point of 30 min registered approximately 88% release of the encapsulated curcumin. Following this initial time point, insignificant change in the release of curcumin was recorded during the following 150 min of digestion time. Within the first 30 min of intestinal digestion, various morphological changes can be observed including some aggregation of MFGs. Bright-field images at 30 min (Fig. 6.A) shows expulsion of oil droplets indicated by blue arrows. Fig. 6.C shows needle-shaped crystals at the peripheral of damaged MFGs structures (red arrows). At the end of the digestion step at 180 min, fewer intact MFGs were observed. Fluorescent images (Fig. 6.D) show localization of curcumin in the digested MFGs structure.

Particle size distribution of MFGs post intestinal digestion is shown in Fig. 4. A peak shift was observed in particle size distribution curve, from approximately 4.4 μm to 17.4 μm, as well as a widening of the particle size distribution. Additionally, a minor secondary peak appeared toward larger diameter particles (>90 μm) indicating formation of large aggregates of MFGs. Increase in $D_{3,4}$, $D_{0.1}$, and $D_{0.9}$ were all statistically significant after intestinal digestion compared to particle size measurements prior to digestion.

4. Discussion:

4.1 Encapsulation of curcumin into milk fat globules

Encapsulation of curcumin is required for many food and drug applications due to the compound's low aqueous solubility of curcumin (11 ng/mL in buffer solution) [36].

This study investigated the feasibility of encapsulating this lipid-soluble bioactive compound in intact MFGs, where MFGs isolated from raw milk were suspended in water then combined with an ethanolic solution of curcumin. The use of ethanol allows dispersion of curcumin in the MFGs aqueous environment, consequently facilitating the interaction of curcumin with MFGs. In addition, ethanol also enhances the partitioning of curcumin through the MFGM due to its ability to increase the permeability of biological membranes [37, 38].

Partitioning of curcumin across the tri-layer membrane of the MFGs and deposition in the lipid core was visualized by CLSM. Fig. 1.B show uniform distribution of the fluorescence signal of the compound in MFGs. Partitioning of curcumin in MFGs can be attributed to curcumin's ability to bind cellular membranes, solubilize and accumulate in biological bilayers, as well as its association with interfacial proteins [39-42]. The binding is facilitated by high hydrophobic characteristics of curcumin represented by relatively high octanol/water partitioning coefficient, i.e. log *P* of 4.3 [2, 3]. Additionally, the work of Barry *et al.* (2009) [43] suggests that the presence of curcumin in the bilayer also increases the permeability of biological membranes. This could partly explain the increase in LC of curcumin with an increase in curcumin concentration in the aqueous phase. Once curcumin partitions into the MFGM, concentration gradient and solubility of curcumin in the lipid phase favors its diffusion to the MFGs core.

The LC values reported in this study (Table 2) likely represent the sum total of curcumin solubilized in the TAG core, accumulated in the bilayer, and associated with the MFGM outer leaflet. These values are much higher than those reported in other natural carriers. Young *et al.* (2017) [20] reported an encapsulation yield of curcumin in

yeast cells of approximately 400 μg of curcumin/g of yeast. On the other hand, typical LC of curcumin in engineered lipid carriers such as emulsions are between 290 and 300 μg/g for curcumin in canola oil or medium chain TAG[44-46], approximately 3 folds lower than LC reported in this study using MFGs carriers.

4.2 Release of curcumin from MFGs under simulated gastrointestinal digestion conditions

Firstly, MFGs were subjected to simulated gastric digestion phase. The gastric phase did not include gastric lipase as limited milk fat digestion is reported in the case of native MFGs coated with MFGM [49-51]. Furthermore, Armand (2008) [52] have reported limited gastric lipase interaction with MFGM due to the presence of phosphatidylethanolamine and sphingomyelin at the interface. In addition, other studies have also reported gastric limited lipase enzymatic activity (< 25%) due to sub-optimal pH values, particularly at fasted state (pH ≤ 3.0) [53-56]. The pH conditions used in this study however were near optimal for pepsin activity [57].

The study of release of curcumin under gastric conditions is important as the release of the poorly water-soluble compound into the acidic aqueous environment of the stomach might result in hydrolysis or precipitation of the compound due to limited solubility in the aqueous phase [36]. Accordingly, carrier structures that are stable under gastric conditions and are able to provide the desired control on enteric release of bioactives such as curcumin are better suited as for the delivery of lipid-soluble compounds [58].

The release of curcumin from MFGs in the gastric phase exhibited a burst release of approximately 17% of encapsulated during the first recorded time point at 30 min. After the initial release no significant increase in the release of curcumin was observed with extended incubation up to 2 h. The initial burst release could be a result of release of superficially bound curcumin associated with MFGM interface including the proteinaceous coating of the membrane. Young (2018) [59] and others[59, 60] reported a limited release of curcumin from yeast cells in gastric fluids (total of 15% in 2 h) exhibiting a similar release profile to that reported in this study. Limited release in the gastric phase was also reported for complex emulsion structures such as Pickering emulsions, Tikekar *et al.* (2013) [31] reported 22% release of curcumin at the end of 2 h simulated gastric digestion. On the other hand, release of curcumin from protein-chitosan-based nanocomplexes was reported to be much higher, reaching up to 65% of the encapsulated value [61].

CLSM of MFGs showed intactness of a large number of MFGs after 120 min of SGD (Fig. 3.C and D), this can be attributed to MFGM and MFGs lipid core resistance to digestion [49]. Additionally, distinct lipid formation can be observed surrounding some of the lipid droplets (red arrow in Fig. 3C). These are believed to be amorphous lipids that appear as protrusions and could potentially represent lamellar phase of lipids that form due to alteration in the MFGM phospholipid-protein interactions resulting from conformational changes and/or digestion of some membrane proteins in the gastric phase [62, 63]. The shift in mean particle diameter (Fig. 4) can be attributed to flocculation of MFGs as reported by Ye *et al.* (2011) [64], which is associated with modification to MFGM

interface such as screening of the electrostatic charge at the interface and digestion of MFGs proteinaceous coating.

Intestinal digestion was carried out without pre-gastric digestion, in the presence of pancreatic lipase and bile salts as the main digestive components. Intestinal lipolysis is essential for the bioaccessibility of lipid-soluble compounds. In the duodenum, triglycerides are digested to monoglycerides and fatty acids that are then micellized with the aid of bile salts and absorbed into the gut. Hence, lipolysis is an essential mechanism for the release and bioaccessibility of encapsulated hydrophobic compounds [65-67]. Therefore, encapsulation systems with maximized intestinal release are associated with increased bioaccessibility hydrophobic encapsulates.

Release of curcumin from MFGs under SID exhibited significant release within the first 30 min of incubation (>80%); additional release up to 180 min was not statistically significant. Release of curcumin from highly complex carriers such as yeast cells under similar intestinal phase conditions was reported to have a similar profile and total of 80% of encapsulated curcumin released in 3 h [59]. On the other hand, the release kinetics of curcumin from Pickering emulsion were reported to be gradual over the course of 3 h in SIF, totaling 55% of the encapsulated curcumin [31]. The implication of limited gastric release and extensive intestinal release could potentially positively affect the bioaccesibility of curcumin. Moreover, the presence of MFGM components such as polar lipids could result in the formation of mixed bile salts, consequently enhancing absorption in the gut [27].

The extent of MFGs morphological changes under SID are evident in the increase of particle size in $D_{3,4}$, $D_{0.1}$, $D_{0.9}$ presented in Table. 3 as well as broadening and shift of

the mean diameter presented in Fig. 4. These changes represent the cumulative result of physical, chemical, and enzymatic effects due to mechanical agitation, elevated temperature, the presence of bio-surfactant (i.e. bile salts) as well as digestive enzymes (i.e. pancreatic lipase). In Fig. 6.A blue arrows highlight oil droplets being expelled from crystalline shell, this phenomena was first observed by Patton and Carey (1979) [68] and more recently by Gallier *et al.* (2012 & 2013) [49, 69]. Needle-shaped crystals in Fig. 6.C are likely composed of free fatty acids resulting from milk fat digestion [69].

Endogenous fluorescence of curcumin in the lipid phase at the end of gastric and intestinal digestion (Fig. 3.D and Fig 6.D) could indicate stability of the compound against hydrolysis. Curcumin is only slightly soluble in water at alkaline pH, and undergoes hydrolysis when in contact with water [70]. This results in quenching of the fluorescence intensity [71].

5. Conclusion

The results of this study confirm the feasibility of encapsulating hydrophobic bioactive compounds into the preformed complex lipid structures, MFGs. Greater than 1000 μg of curcumin were encapsulated per gram of milk fat in the form of MFGs via simple diffusion driven by hydrophobic affinity of curcumin. This simple method enables at least 3 folds increase in encapsulation yield of curcumin compared to the reported loading values in emulsions formed using edible oils. *In vitro* release of curcumin from MFGs carriers exhibited minimal release in gastric phase (approximately 27% in 2 h), and extensive release under intestinal conditions (>80%). These results suggest that MFGs carrier could be used successfully for encapsulation and oral delivery of lipid-

soluble compounds.

Funding

Ms. Alshehab was funded by Kuwait University Graduate Study Fellowship. This research was also supported by funding from the USDA-NIFA Foundational Food Quality Program.

Supplementary material

To validate the integrity of milk fat globule member in the presence of 10% v/v ethanol in the continuous aqueous phase, the MFGM was probed with a fluorescently labeled phosphoethanolamine (Oregon Green™ 488 DHPE was purchased from Thermo Fisher Scientific Waltham, MA, U.S.A.). To summarize, the label was prepared in chloroform (1 mg/mL), then 2.5 µl of the label was added to 1 mL of MFGs suspended in water and allowed to incubate for 10 min in the dark. Ethanol was then added at 10% v/v and incubated for no less than 10 minutes. For imaging purposes, a small amount of glycerol was added to the mixture reduce the rate of motion of the globules. Confocal laser scanning microscopy (CLSM) images were collected on Leica TCS SP8 STED 3X fitted with 40x/1.1 water HC PL APO CS2 objective (Buffalo Grove, IL, U.S.A.). Excitation and emission were set as 488 nm and 580 nm respectively. Fluorescence emission was collected on Hyd 2 detector at standard mode (499 nm – 591 nm), bright field images were collected using PMT Trans detector.

References

1. Kitts DD. Bioactive substances in food: Identification and potential uses. Can J Physiol Pharmacol. 1994;72(4):423-34.

2. Yamagami C, Araki K, Ohnishi K, Hanasato K, Inaba H, Aono M, et al. Measurement and prediction of hydrophobicity parameters for highly lipophilic compounds: Application of the hplc column‐switching technique to measurement of log p of diarylpyrazines. J Pharm Sci. 1999;88(12):1299-304.

3. Nakayama T, ONo K, HAsHiMoTo K. Affinity of antioxidative polyphenols for lipid bilayers evaluated with a liposome system. Biosci, Biotechnol, Biochem. 1998;62(5):1005-7.

4. Aggarwal BB, Harikumar KB. Potential therapeutic effects of curcumin, the anti-inflammatory agent, against neurodegenerative, cardiovascular, pulmonary, metabolic, autoimmune and neoplastic diseases. Int J Biochem Cell Biol. 2009;41(1):40-59.

5. Ak T, Gülçin İ. Antioxidant and radical scavenging properties of curcumin. Chem-Biol Interact. 2008;174(1):27-37.

6. Swamy MV, Citineni B, Patlolla JM, Mohammed A, Zhang Y, Rao CV. Prevention and treatment of pancreatic cancer by curcumin in combination with omega-3 fatty acids. Nutr Cancer. 2008;60(S1):81-9.

7. Dhillon N, Aggarwal BB, Newman RA, Wolff RA, Kunnumakkara AB, Abbruzzese JL, et al. Phase ii trial of curcumin in patients with advanced pancreatic cancer. Clin Cancer Res. 2008;14(14):4491-9.

8. Condat M, Mazeran P-E, Malval J-P, Lalevée J, Morlet-Savary F, Renard E, et al. Photoinduced curcumin derivative-coatings with antibacterial properties. RSC Advances. 2015;5(104):85214-24.

9. Mun S-H, Joung D-K, Kim Y-S, Kang O-H, Kim S-B, Seo Y-S, et al. Synergistic antibacterial effect of curcumin against methicillin-resistant staphylococcus aureus. Phytomedicine. 2013;20(8-9):714-8.

10. Tyagi P, Singh M, Kumari H, Kumari A, Mukhopadhyay K. Bactericidal activity of curcumin i is associated with damaging of bacterial membrane. PLoS ONE. 2015;10(3):e0121313.

11. Mei L, McClements DJ, Wu J, Decker EA. Iron-catalyzed lipid oxidation in emulsion as affected by surfactant, ph and nacl. Food Chem. 1998;61(3):307-12.

12. Mei L, McClements DJ, Decker EA. Lipid oxidation in emulsions as affected by charge status of antioxidants and emulsion droplets. J Agric Food Chem. 1999;47(6):2267-73.

13. Warren DB, Chalmers DK, Hutchison K, Dang W, Pouton CW. Molecular dynamics simulations of spontaneous bile salt aggregation. Colloids Surf Physicochem Eng Aspects. 2006;280(1-3):182-93.

14. Charoen R, Jangchud A, Jangchud K, Harnsilawat T, Naivikul O, McClements DJ. Influence of biopolymer emulsifier type on formation and stability of rice bran oil‐in‐water emulsions: Whey protein, gum arabic, and modified starch. J Food Sci. 2011;76(1):E165-E72.

15. Dickinson E. Hydrocolloids as emulsifiers and emulsion stabilizers. Food Hydrocoll. 2009;23(6):1473-82.

16. Pannell N. Microbial encapsulation. European Patent 1990;242:135.

17. Czerniak A, Kubiak P, Białas W, Jankowski T. Improvement of oxidative stability of menhaden fish oil by microencapsulation within biocapsules formed of yeast cells. J Food Eng. 2015;167:2-11.

18. Paukner S, Kohl G, Lubitz W. Bacterial ghosts as novel advanced drug delivery systems: Antiproliferative activity of loaded doxorubicin in human caco-2 cells. J Controlled Release. 2004;94(1):63-74.

19. Hamidi M, Zarrin A, Foroozesh M, Mohammadi-Samani S. Applications of carrier erythrocytes in delivery of biopharmaceuticals. J Controlled Release. 2007;118(2):145-60.

20. Young S, Dea S, Nitin N. Vacuum facilitated infusion of bioactives into yeast microcarriers: Evaluation of a novel encapsulation approach. Food Res Int. 2017;100:100-12.

21. Rohlfs EM, Louie DS, Zeisel SH. Lipid synthesis and secretion by primary cultures of rat mammary epithelial cells. J Cell Physiol. 1993;157(3):469-80.

22. Fox PF, McSweeney PLH. Advanced dairy chemistry: Springer; 2014.

23. McManaman JL. Formation of milk lipids: A molecular perspective. Journal of Clinical Lipidology 2009;4(3):391-401.

24. Michalski MC. Specific molecular and colloidal structures of milk fat affecting lipolysis, absorption and postprandial lipemia. Eur J Lipid Sci Technol. 2009;111(5):413-31.

25. MacGibbon A, Taylor M. Composition and structure of bovine milk lipids. Advanced dairy chemistry volume 2 lipids: Springer; 2006. p. 1-42.

26. Berton‐Carabin CC, Ropers MH, Genot C. Lipid oxidation in oil‐in‐water emulsions: Involvement of the interfacial layer. Comprehensive Reviews in Food Science and Food Safety. 2014;13(5):945-77.

27. Liu H-X, Adachi I, Horikoshi I, Ueno M. Mechanism of promotion of lymphatic drug absorption by milk fat globule membrane. Int J Pharm. 1995;118(1):55-64.

28. Kanno C. Emulsifying properties of bovine milk fat globule membrane in milk fat emulsion: Conditions for the reconstitution of milk fat gobules. J Food Sci. 1989;54(6):1534–9.

29. Farhang B. Encapsulation of bioactive compounds in liposomes prepared with milk fat globule membrane-derived phospholipids. Guelph, Ontario, Canada: The University of Guelph; 2013.

30. Gallier S, Gragson D, Jimenez-Flores R, Everett D. Using confocal laser scanning microscopy to probe the milk fat globule membrane and associated proteins. J Agric Food Chem. 2010;58(7):4250-7.

31. Tikekar RV, Pan Y, Nitin N. Fate of curcumin encapsulated in silica nanoparticle stabilized pickering emulsion during storage and simulated digestion. Food Res Int. 2013;51(1):370-7.

32. Sarkar A, Goh KKT, Singh RP, Singh H. Behaviour of an oil-in-water emulsion stabilized by β-lactoglobulin in an in vitro gastric model. Food Hydrocoll. 2009;23(6):1563-9.

33. Minekus M, Alminger M, Alvito P, Ballance S, Bohn T, Bourlieu C, et al. A standardised static in vitro digestion method suitable for food - an international consensus. Food & Function. 2014;5(6):1113-24.

34. Sarkar A, Horne DS, Singh H. Interactions of milk protein-stabilized oil-in-water emulsions with bile salts in a simulated upper intestinal model. Food Hydrocoll. 2010;24(2-3):142-51.

35. Porter CJ, Trevaskis NL, Charman WN. Lipids and lipid-based formulations: Optimizing the oral delivery of lipophilic drugs. Nature Reviews Drug Discovery. 2007;6(3):231-48.

36. Tønnesen HH, Másson M, Loftsson T. Studies of curcumin and curcuminoids. Xxvii. Cyclodextrin complexation: Solubility, chemical and photochemical stability. Int J Pharm. 2002;244(1-2):127-35.

37. Ingram LO. Ethanol tolerance in bacteria. Crit Rev Biotechnol. 1989;9(4):305-19.

38. Komatsu H, Okada S. Effects of ethanol on permeability of phosphatidylcholine/cholesterol mixed liposomal membranes. Chem Phys Lipids. 1997;85(1):67-74.

39. Bourassa P, Kanakis C, Tarantilis P, Pollissiou M, Tajmir-Riahi H. Resveratrol, genistein, and curcumin bind bovine serum albumin. J Phys Chem B. 2010;114(9):3348-54.

40. Jaruga E, Sokal A, Chrul S, Bartosz G. Apoptosis-independent alterations in membrane dynamics induced by curcumin. Exp Cell Res. 1998;245(2):303-12.

41. Khajavi M, Shiga K, Wiszniewski W, He F, Shaw CA, Yan J, et al. Oral curcumin mitigates the clinical and neuropathologic phenotype of the trembler-j mouse: A potential therapy for inherited neuropathy. The American Journal of Human Genetics. 2007;81(3):438-53.

42. Sun Y, Lee C-C, Hung W-C, Chen F-Y, Lee M-T, Huang HW. The bound states of amphipathic drugs in lipid bilayers: Study of curcumin. Biophys J. 2008;95(5):2318-24.

43. Barry J, Fritz M, Brender JR, Smith PE, Lee D-K, Ramamoorthy A. Determining the effects of lipophilic drugs on membrane structure by solid-state nmr spectroscopy: The case of the antioxidant curcumin. J Am Chem Soc. 2009;131(12):4490-8.

44. Pan Y, Tikekar RV, Nitin N. Effect of antioxidant properties of lecithin emulsifier on oxidative stability of encapsulated bioactive compounds. Int J Pharm. 2013;450(1-2):129-37.

45. Kharat M, Du Z, Zhang G, McClements DJ. Physical and chemical stability of curcumin in aqueous solutions and emulsions: Impact of ph, temperature, and molecular environment. J Agric Food Chem. 2017;65(8):1525-32.

46. McClements DJ. Crystals and crystallization in oil-in-water emulsions: Implications for emulsion-based delivery systems. Adv Colloid Interface Sci. 2012;174:1-30.

47. Armand M, Borel P, Pasquier B, Dubois C, Senft M, Andre M, et al. Physicochemical characteristics of emulsions during fat digestion in human stomach and duodenum. Am J Physiol Gastrointest Liver Physiol. 1996;271(1):G172-G83.

48. Mun S, Decker EA, Park Y, Weiss J, McClements DJ. Influence of interfacial composition on in vitro digestibility of emulsified lipids: Potential mechanism for chitosan's ability to inhibit fat digestion. Food Biophys. 2006;1(1):21-9.

49. Gallier S, Ye A, Singh H. Structural changes of bovine milk fat globules during in vitro digestion. J Dairy Sci. 2012;95(7):3579-92.

50. Roman C, Carriere F, Villeneuve P, Pina M, Millet V, Simeoni U, et al. Quantitative and qualitative study of gastric lipolysis in premature infants: Do mct-enriched infant formulas improve fat digestion? Pediatr Res. 2007;61(1):83.

51. Bernbäck S, Bläckberg L, Hernell O. Fatty acids generated by gastric lipase promote human milk triacylglycerol digestion by pancreatic colipase-dependent lipase. Biochimica et Biophysica Acta, Lipids and Lipid Metabolism. 1989;1001(3):286-93.

52. Armand M. Milk fat digestibility. Sciences des Aliments. 2008;28(1-2):84-98.

53. Gargouri Y, Pieroni G, Lowe PA, Sarda L, Verger R. Human gastric lipase: The effect of amphiphiles. Eur J Biochem. 1986;156(2):305-10.

54. Gargouri Y, Moreau H, Verger R. Gastric lipases: Biochemical and physiological studies. Biochimica et Biophysica Acta, Lipids and Lipid Metabolism. 1989;1006(3):255-71.

55. Hamosh M, Scanlon JW, Ganot D, Likel M, Scanlon KB, Hamosh P. Fat digestion in the newborn: Characterization of lipase in gastric aspirates of premature and term infants. J Clin Invest. 1981;67(3):838-46.

56. Dressman JB, Berardi RR, Dermentzoglou LC, Russell TL, Schmaltz SP, Barnett JL, et al. Upper gastrointestinal (gi) ph in young, healthy men and women. Pharm Res. 1990;7(7):756-61.

57. Piper D, Fenton BH. Ph stability and activity curves of pepsin with special reference to their clinical importance. Gut. 1965;6(5):506.

58. Suwannateep N, Banlunara W, Wanichwecharungruang SP, Chiablaem K, Lirdprapamongkol K, Svasti J. Mucoadhesive curcumin nanospheres: Biological activity, adhesion to stomach mucosa and release of curcumin into the circulation. J Controlled Release. 2011;151(2):176-82.

59. Young S. The physicochemical properties of yeast microcarriers: University of California, Davis; 2018.

60. Paramera EI, Konteles SJ, Karathanos VT. Stability and release properties of curcumin encapsulated in saccharomyces cerevisiae, β-cyclodextrin and modified starch. Food Chem. 2011;125(3):913-22.

61. Zhou M, Hu Q, Wang T, Xue J, Luo Y. Characterization of high density lipoprotein from egg yolk and its ability to form nanocomplexes with chitosan as natural delivery vehicles. Food Hydrocoll. 2018;77:204-11.

62. Gallier S, Cui J, Olson TD, Rutherfurd SM, Ye A, Moughan PJ, et al. In vivo digestion of bovine milk fat globules: Effect of processing and interfacial structural changes. I. Gastric digestion. Food Chem. 2013;141(3):3273-81.

63. Vanderghem C, Francis F, Danthine S, Deroanne C, Paquot M, Pauw ED, et al. Study on the susceptibility of the bovine milk fat globule membrane proteins to enzymatic hydrolysis and organization of some of the proteins. Int Dairy J. 2011;21(5):312–8.

64. Ye A, Cui J, Singh H. Proteolysis of milk fat globule membrane proteins during in vitro gastric digestion of milk. J Dairy Sci. 2011;94(6):2762-70.

65. Pool H, Mendoza S, Xiao H, McClements DJ. Encapsulation and release of hydrophobic bioactive components in nanoemulsion-based delivery systems: Impact of physical form on quercetin bioaccessibility. Food & Function. 2013;4(1):162-74.

66. Yao M, Xiao H, McClements DJ. Delivery of lipophilic bioactives: Assembly, disassembly, and reassembly of lipid nanoparticles. Annu Rev Food Sci Technol. 2014;5:53-81.

67. McClements DJ, Saliva-Trujillo L, Zhang R, Zhang Z, Zou L, Yao M, et al. Boosting the bioavailability of hydrophobic nutrients, vitamins, and nutraceuticals in natural products using excipient emulsions. Food Res Int. 2015.

68. Patton JS, Carey MC. Watching fat digestion. Science. 1979;204(4389):145-8.

69. Gallier S, Zhu XQ, Rutherfurd SM, Ye A, Moughan PJ, Singh H. In vivo digestion of bovine milk fat globules: Effect of processing and interfacial structural changes. Ii. Upper digestive tract digestion. Food Chem. 2013;141(3):3215-23.

70. Bong PH. Spectral and photophysical behaviors of curcumin and curcuminoids. Bull Korean Chem Soc. 2000;21(1):81-6.

71. Priyadarsini KI. Photophysics, photochemistry and photobiology of curcumin: Studies from organic solutions, bio-mimetics and living cells. J Photochem Photobiol C: Photochem Rev. 2009;10(2):81-95.

Tables

Incubation time (min)	EE%
10	62.36±1.85
20	66.43±4.32
30	61.20±1.78
40	59.75±2.10
50	57.24±0.83*
60	64.30±2.42

Table 1: The effect of incubation time on the EE% of curcumin in MFGs. * Denotes values which are significantly different ($p < 0.05$).

Concentration of added curcumin/cream (µg/g)	v/v % of ethanol	EE%	LC%, curcumin/milk fat (µg/g)
200	1	62.09±1.46	368.11±2.92 [a]
400	2	61.17±2.13	244.69±8.53 [b]
600	3	62.10±2.54	372.60±15.27 [c]
1000	5	66.56±0.13*	665.55±1.31 [d]
1600	8	62.55±0.37	1000.76±5.97 [e]
2000	10	59.33±0.73	1186.65±14.63 [e]

Table 2: The effects of curcumin and ethanol concentrations on the EE% and LC% into MFGs and reported per g of milk fat. Fat content was measured to be 4.71±0.29 g/ 10 g of cream. EE, encapsulation efficiency; LC. loading capacity. Different letters and * denotes values which are significantly differe ($p < 0.05$).

Time (min)	MFGs particle size distribution (μm)		
	Volume mean diameter, $D_{4,3}$	10th percentile diameter , $D_{0.1}$	90th percentile diameter, $D_{0.9}$
Prior to digestion	4.58±0.40	2.02±0.14	7.75±0.87
Simulated gastric digestion			
30	5.92±0.16 [a]	2.75±0.12 [a]	10.01±0.38 [a]
60	6.58±0.16 [b]	2.89±0.21 [b]	11.10±0.23 [b]
90	6.83±0.15 [c]	3.34±0.29 [c]	11.34±0.13 [c]
120	7.42±0.20 [d]	3.63±0.32 [d]	12.42±0.29 [d]
Simulated intestinal digestion			
30	27.85±5.15 [a]	6.22±1.63 [a]	114.87±52.42 [a]
60	24.53±4.86 [b]	6.15±1.57 [b]	67.24±28.37 [b]
90	35.85±16.92 [c]	6.52±1.23 [c]	94.55±34.40 [c]
120	27.52±6.86 [d]	6.41±1.09 [d]	98.10±36.34 [d]
150	26.56±4.14 [e]	6.24±1.15 [e]	72.66±23.05 [e]
180	32.27±13.17 [f]	5.86±1.45 [f]	80.17±40.13 [f]

Table 3: MFGs diameter as a function of digestion time. Different letters indicate statistically significant difference within each column in comparison the particle size prior to digestion ($p < 0.05$).

Figures captions

Figure 1: Confocal laser scanning microscopy showing the partitioning of curcumin into MFGs after 10 minutes incubation. A) bright field image of MFGs with encapsulated curcumin, B) fluorescence images of curcumin in MFGs.

Figure 2: Release of curcumin encapsulated in MFGs under simulated gastric conditions.

Figure 3: Confocal laser scanning microscopy images of MFGs with encapsulated curcumin during simulated gastric digestion. A-B) After 30 min of SGD, MFGs appear spherical and intact with uniformly distributed fluorescence signal of curcumin. C) Bright field image of MFGs after 120 min of SGD, red arrows point at Irregular boundaries of the lipid droplets. SGD, simulated gastric digestion crystalline lipids.

Figure 4: MFGs diameter distribution prior to digestion (circle), post gastric digestion (square), and post intestinal digestion (triangle).

Figure 5: Release of curcumin encapsulated in MFGs under simulated intestinal digestion conditions.

Figure 6: Confocal laser scanning microscopy images of MFGs with encapsulated curcumin during simulated intestinal digestion. A) Bright field images captured after 30 min of SID, blue arrow point at oil droplets being expelled, red arrows in point at amorphous lipids. C) Red arrows point in at needle-shaped structures. B and D)

Fluorescence images at 30 and 180 min respectively, fluorescence signal indicate presence of curcumin. SID, simulated intestinal digestion.

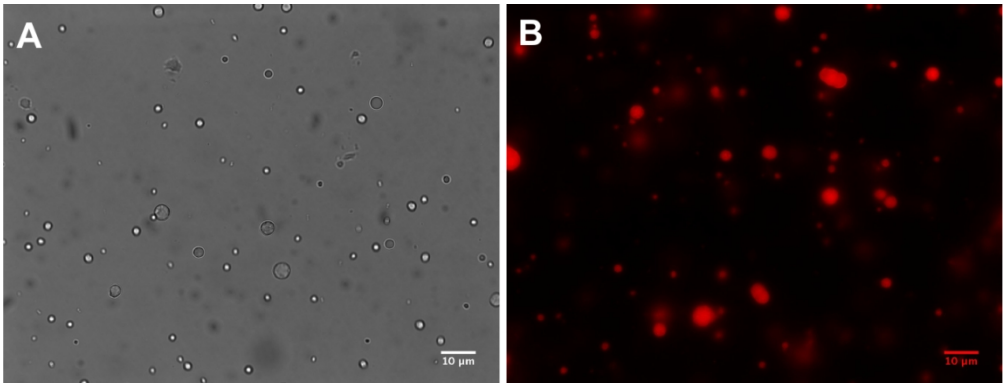

Figure 1: Confocal laser scanning microscopy showing the partitioning of curcumin into MFGs after 10 minutes incubation. A) bright field image of MFGs with encapsulated curcumin, B) fluorescence images of curcumin in MFGs.

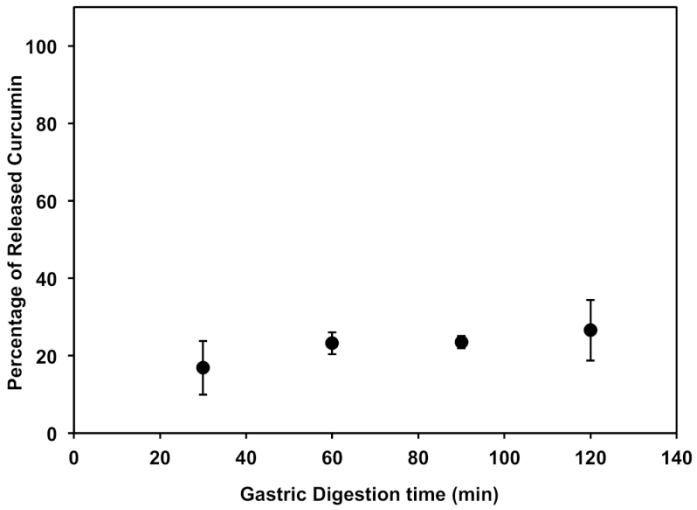

Figure 2: Release of curcumin encapsulated in MFGs under simulated gastric digestion conditions.

705x529mm (72 x 72 DPI)

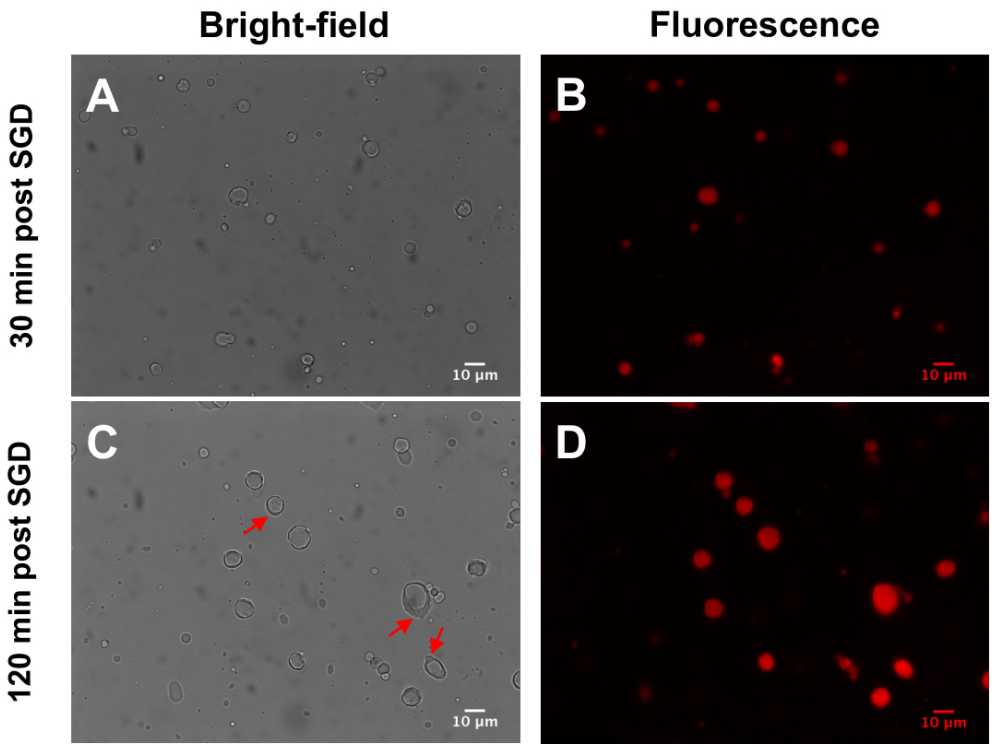

Figure 3: Confocal laser scanning microscopy images of MFGs with encapsulated curcumin during simulated gastric digestion. A-B) After 30 min of SGD, MFGs appear spherical and intact with uniformly distributed fluorescence signal of curcumin. C) Bright field image of MFGs after 120 min of SGD, red arrows point at Irregular boundaries of the lipid droplets. SGD, simulated gastric digestion crystalline lipids.

382x288mm (72 x 72 DPI)

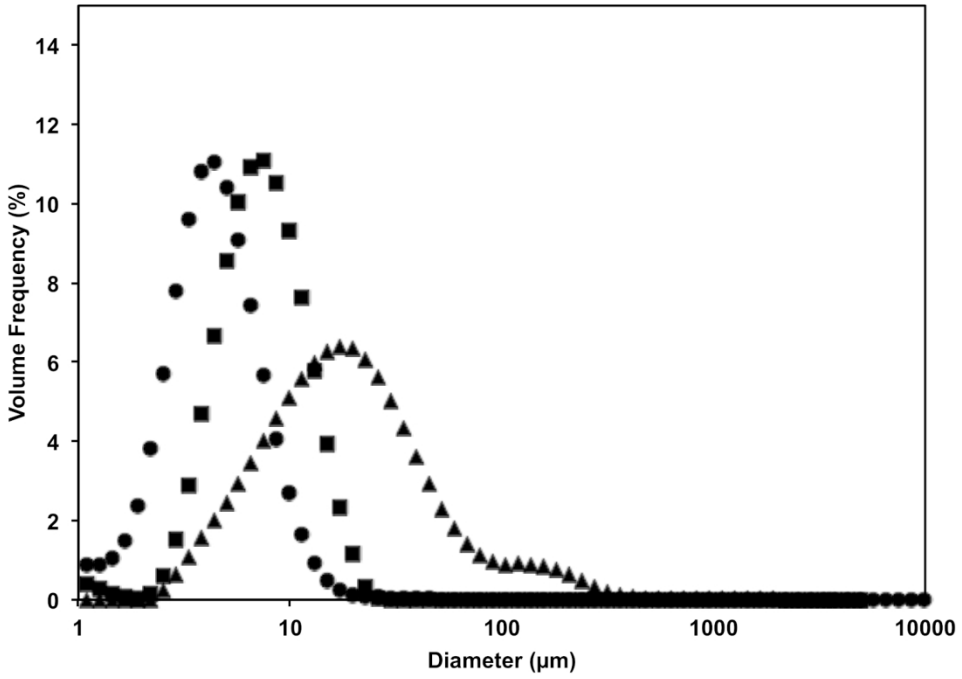

Figure 4: MFGs diameter distribution prior to digestion (circle), post gastric digestion (square), and post intestinal digestion (triangle).

615x440mm (72 x 72 DPI)

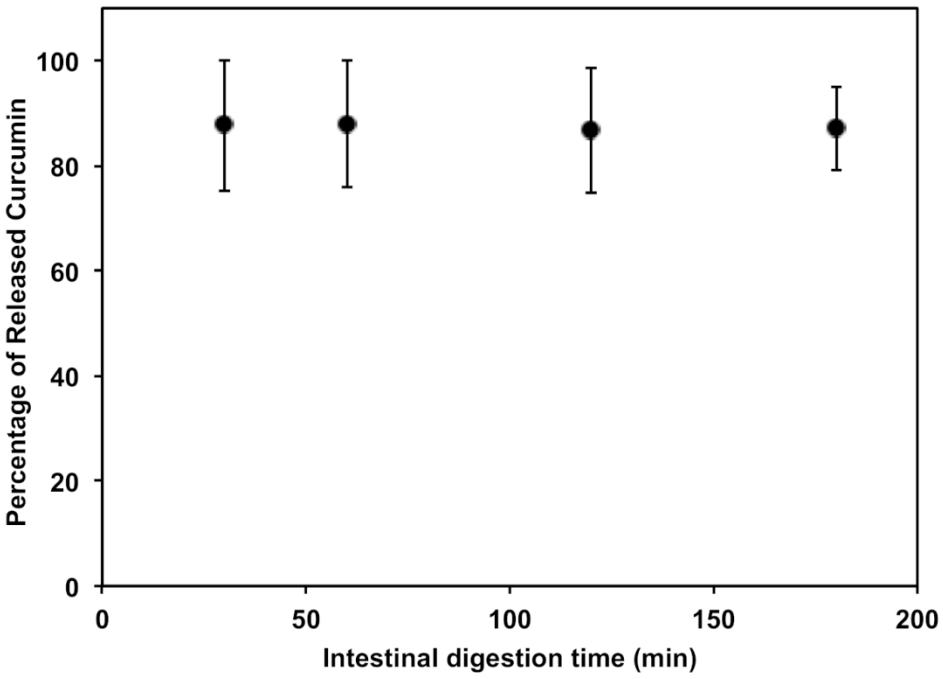

Figure 5: Release of curcumin encapsulated in MFGs under simulated intestinal conditions.

518x390mm (72 x 72 DPI)

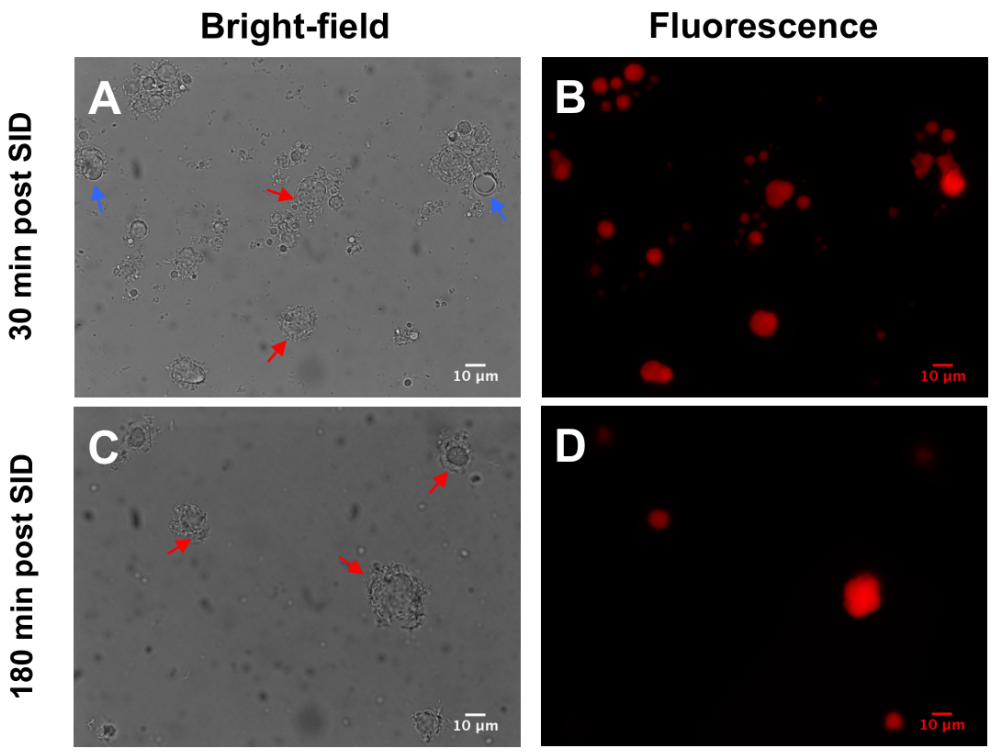

Figure 6: Confocal laser scanning microscopy images of MFGs with encapsulated curcumin during simulated intestinal digestion. A) Bright field images captured after 30 min of SID, blue arrow point at oil droplets being expelled, red arrows in point at amorphous lipids. C) Red arrows point in at needle-shaped structures. B and D) Fluorescence images at 30 and 180 min respectively, fluorescence signal indicate presence of curcumin. SID, simulated intestinal digestion.

384x291mm (72 x 72 DPI)

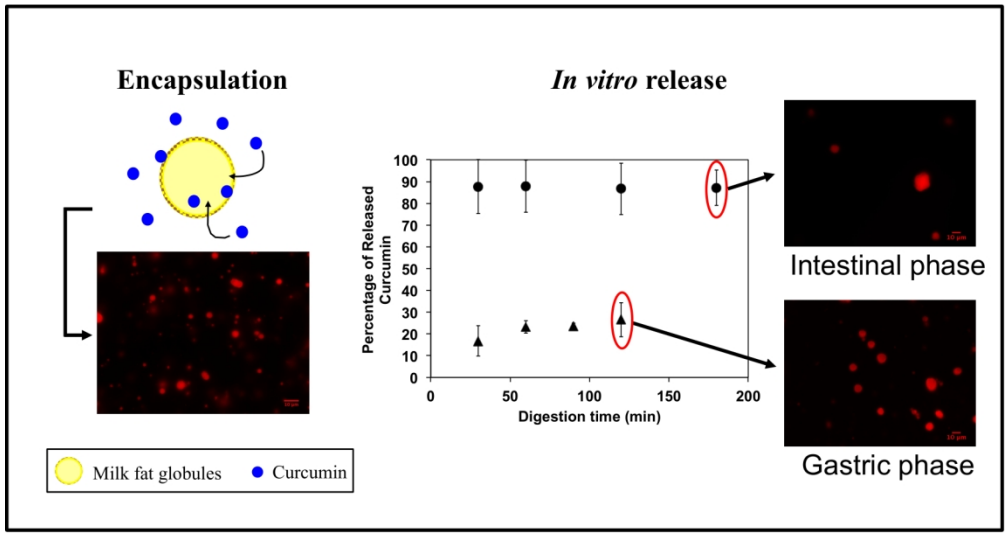

629x332mm (72 x 72 DPI)